17th World Conference on Earthquake Engineering, 17WCEE
Sendai, Japan - September 27th to October 2nd 2021

SEISMIC ISOLATION OF SAFETY-CLASS EQUIPMENT IN ADVANCED NUCLEAR POWER PLANTS

K. M. Lal[(1)], A. S. Whittaker [(2)], M. C. Constantinou[(3)]

[(1)] *Ph.D. Student, Department of Civil, Structural and Environmental Engineering, University at Buffalo, The State University of New York, Buffalo, NY, USA, klal@buffalo.edu*
[(2)] *SUNY Distinguished Professor, Department of Civil, Structural and Environmental Engineering, University at Buffalo, The State University of New York, Buffalo, NY, USA, awhittak@buffalo.edu*
[(3)] *SUNY Distinguished Professor, Department of Civil, Structural and Environmental Engineering, University at Buffalo, The State University of New York, Buffalo, NY, USA, constan1@buffalo.edu*

Abstract

Seismic isolation can substantially reduce earthquake loadings on structures, systems, components (SSCs), and equipment, and is being considered for application to advanced nuclear reactors. The conventional implementation isolates the reactor building at its base and was the focus of several completed research projects funded by the U.S. Department of Energy (DOE) and U.S. Nuclear Regulatory Commission (NRC). An alternate implementation of seismic isolation involves protection of SSCs and equipment inside a reactor building, which is the focus of an on-going MEITNER project funded by the DOE Advanced Research Projects Agency – Energy (ARPA-E).

The MEITNER project includes an experimental program that is investigating the application of seismic isolation to equipment. Four models are being evaluated, with three isolated at the base, and one isolated at its mid-height. This paper presents data on the seismic response of a cylindrical vessel isolated at its mid-height. The test specimen was 240 inches tall and had an outer diameter of 60 inches. The vessel was supported on a stiff steel frame by three equally spaced mounts. Friction Pendulum bearings were installed between each mount and the steel frame. The test specimen was subjected to three component ground motions using a 6 DOF earthquake simulator. The vessel was filled with water and sample internals were attached to the vessel head. Three configurations were tested, non-isolated, isolated using single Friction Pendulum bearings, and isolated using triple Friction Pendulum bearings. Data from the experiments show that mid-height isolation enables significant reductions in seismic demands in both the vessel and its internals.

Keywords: seismic isolation; equipment isolation; safety-class equipment; earthquake simulator testing

1. Introduction

Recent studies have shown that the seismic load case can substantially increase the overnight capital cost (OCC) of safety-class equipment in advanced nuclear reactors [1-3]. Substantial reductions in cost may be realized if safety-class equipment is isolated, because seismic demands are significantly reduced, but this has yet to be proven by physical experiments.

Although seismic isolation has not been used to protect individual pieces of safety-class equipment in a nuclear power plant, its use for non-nuclear applications has been studied, with a focus on power transformers. Murota *et al.* (2005) [4] tested power transformers base isolated using a combined sliding-rubber bearing isolation system. Oikonomou *et al.* (2012) [5] conducted earthquake simulator experiments on a model of a power transformer, base isolated by lead rubber bearings and by triple Friction Pendulum bearings. The successful outcomes of the Oikonomou *et al.* studies led Bonneville Power Administration (BPA) to base isolate an existing high voltage transformer in 2013 and Seattle City Light (SCL) to base isolate a new high voltage power transformer in 2014 [6]. Both applications used triple Friction Pendulum bearings.

The DOE Advanced Research Projects Agency – Energy (ARPA-E) funded an on-going MEITNER project that has the goal of reducing the overnight capital cost of advanced reactors using equipment-level seismic protective systems. The MEITNER project includes proof-of-concept experiments on seismically isolated equipment. Earthquake simulator experiments were performed on four different models. Three of the models were base isolated. The fourth model, described in this paper, was isolated at its mid-height. The cylindrical model in this study, with an aspect ratio of four, could represent a steam generator or a reactor vessel. The vessel was supported on a stiff steel frame and subjected to three component ground motions using a six degrees-of-freedom earthquake simulator at the University at Buffalo. Friction Pendulum isolators, one of the three types of bearings identified in Kammerer *et al*. (2019) [7] and described in ASCE/SEI 4-16 [8] and ASCE/SEI 43-19 [9], were used to isolate the vessel. Two types of Friction Pendulum isolators were utilized: single concave Friction Pendulum (SFP) isolators and triple Friction Pendulum (TFP) isolators. The vessel was filled with water and sample internals were attached to the head of the vessel to characterize the interaction of the fluid, the internals, and the vessel.

2. Test Specimen

The cylindrical, carbon steel test specimen was 240 inches tall, with an outer diameter of 60 inches and a wall thickness of 1 inch. It was supported at its mid-height on a stiff steel frame by three mounts separated by 120 degrees. The mounts were connected via shaped plates welded to the vessel wall to achieve diaphragm action at the isolation plane. The steel frame had overall plan dimensions of 116 in × 116 in and was 120 inches tall. The frame had four outer columns concentrically braced with angle sections providing lateral stiffness, and three inner columns, one beneath each mount, to provide vertical stiffness. Fig.1 presents the test assembly installed on the earthquake simulator, including close-up views of the installed isolators. The vessel was filled with water. A rectangular plate, identified as the vessel head in Fig.1, was bolted to the top of the specimen to attach sample internals and prevent loss of water during testing. Two internals were attached to the vessel head: a 72-inch tall steel plate, with plan dimensions of 0.5 in × 6 in and a first mode frequency in air of about 3 Hz [10], and a 72-inch tall aluminum pipe, with a 3-inch outer diameter, a wall thickness of 1/8 inch, and a first mode frequency in air of about 7 Hz [10]. The total weight of the vessel including the water, head, and internals was approximately 40 kips.

3. Seismic isolation

3.1. Description

Two types of Friction Pendulum bearings were considered for the seismic isolation of the vessel: single concave Friction Pendulum (SFP) bearings and triple Friction Pendulum (TFP) bearings. The SFP bearings consist of an articulated slider coated with a PTFE-type composite, a sliding surface of polished stainless steel, and a housing plate. Fig.2 presents the cross section and internal construction of the SFP bearings. The SFP bearings had a sliding period of 1.38 seconds (frequency of 0.72 Hz) and a displacement capacity of 3.5 inches.

The TFP bearings consist of two concave plates and a nested slider assembly. The slider assembly consists of two concave slide plates separated by a rigid slider and is encased by a rubber seal. The surfaces of the slide plates in contact with the outer concave plates and the two concave surfaces of the rigid slider are coated with a PTFE-type material. Sliding is permitted on all four concave surfaces, which are made of polished stainless steel. Fig.3 presents the cross section and internal construction of the TFP bearings. The concave surfaces in a TFP bearing are numbered 1 through 4 in Fig.3a. The TFP bearings had a sliding

period (for sliding on outer concave surfaces) of 1.96 seconds (frequency of 0.51 Hz) and a displacement capacity of about 6.5 inches.

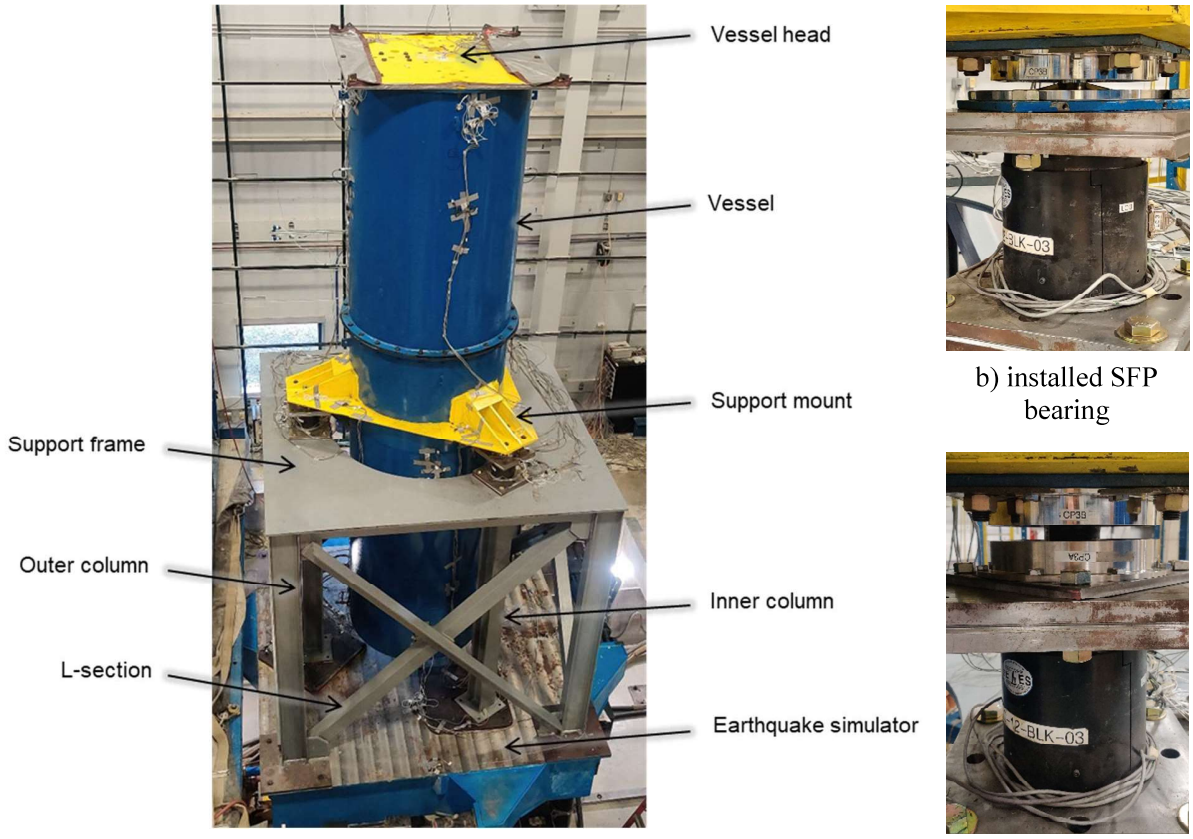

a) isometric view

b) installed SFP bearing

c) installed TFP bearing

Fig. 1 – Test setup on earthquake simulator

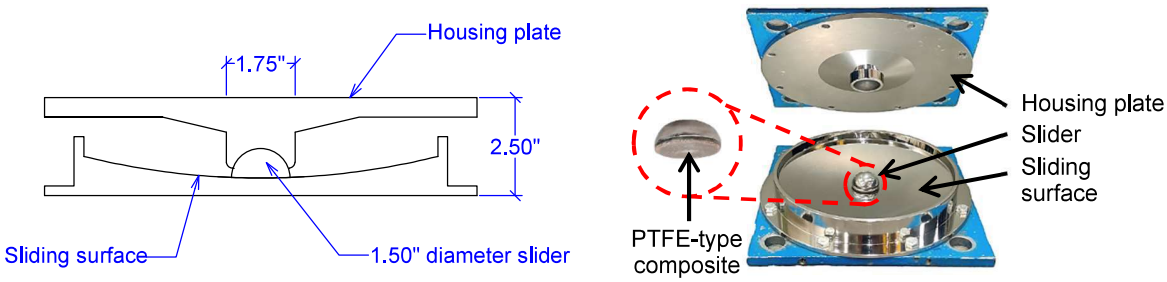

a) cross section

b) internal construction

Fig. 2 – SFP bearing

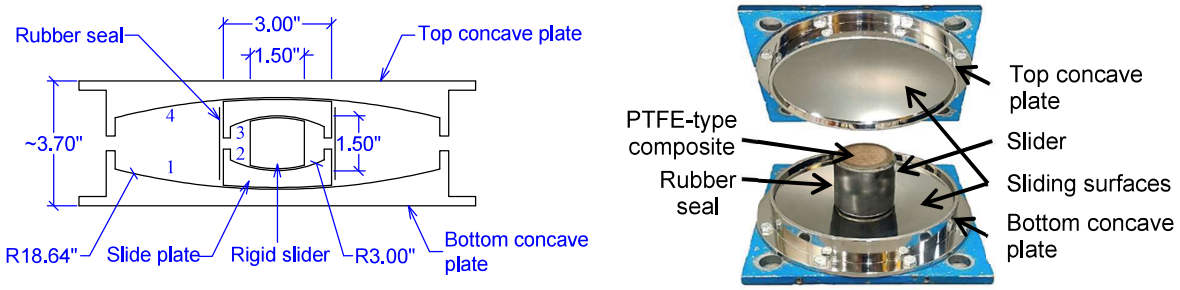

a) cross section b) internal construction

Fig. 3 – TFP bearing

3.2. Characterizing the Friction Pendulum bearings

The horizontal force-displacement behavior of a Friction Pendulum bearing is characterized by the coefficients of friction at the sliding surfaces and the radii of curvature of the sliding surfaces. The mathematical formulation of the force-displacement relationship of Frictional Pendulum bearings is presented in Fenz and Constantinou (2008) [11] and is not repeated here. The radius of curvature of a concave surface is a geometric property and is known a priori. The coefficient of friction at the sliding interface, which is a function of the velocity of the slider, axial pressure on the bearing, and the temperature at the sliding interface, is determined by testing.

To determine the coefficients of friction, the Friction Pendulum bearings were tested under combined axial and unidirectional shear loads in a test machine at the University at Buffalo. The axial and horizontal loads on the bearing and the sliding velocity in the characterization tests were similar to those expected in the earthquake simulator tests. Using the test data, the coefficients of friction were determined using the procedure outlined in Constantinou *et al.* (2007) [12] and the values are reported in Table 1 below.

Table 1 – Coefficients of friction (%) for SFP and TFP bearings

	SFP		TFP			
			$\mu_2 = \mu_3$		$\mu_1 = \mu_4$	
	μ_{slow}	μ_{fast}	*slow*[1]	*fast*[1]	*slow*[1]	*fast*[1]
Bearing 1	2.8	7.6	0.8	2.0	6.8	11.0
Bearing 2	2.7	7.6	0.5	1.5	6.3	11.5
Bearing 3	3.0	8.4	1.0	2.0	7.1	11.3

1. *Slow* and *fast* characterize the velocity of the slider

4. Instrumentation

The response quantities of interest in the proof-of-concept experiments included strains, and accelerations at different elevations on the vessel and the internals, forces and displacements in the bearings, and hydrodynamic pressure and horizontal displacements at discrete locations along on the vessel height. Fig.4 presents the locations of instruments on the vessel and internals. Accelerometers were placed at the top and

bottom of the vessel, and at its mid-height on the support mounts. String potentiometers measured the horizontal displacements at the top, bottom, and mid-height of the vessel with respect to a reference frame on the ground. Hydrodynamic pressures on the vessel wall were measured using pressure gages, placed in arrays of four at three elevations. The forces in the bearings were measured using calibrated five-channel load cells, placed beneath the bearings. The displacements of the bearings were measured using string potentiometers. Accelerometers were installed on the shake table to measure the applied seismic inputs. Accelerometers were also installed at the load cell-bearing interfaces to measure accelerations below the isolation system and atop the steel frame.

Two internals (shaded in green in Fig.4a) were mounted on the vessel head. For each internal, waterproof accelerometers were installed at the mid-height and the bottom. Strains near the points of attachment of the internals were measured using waterproof strain gages.

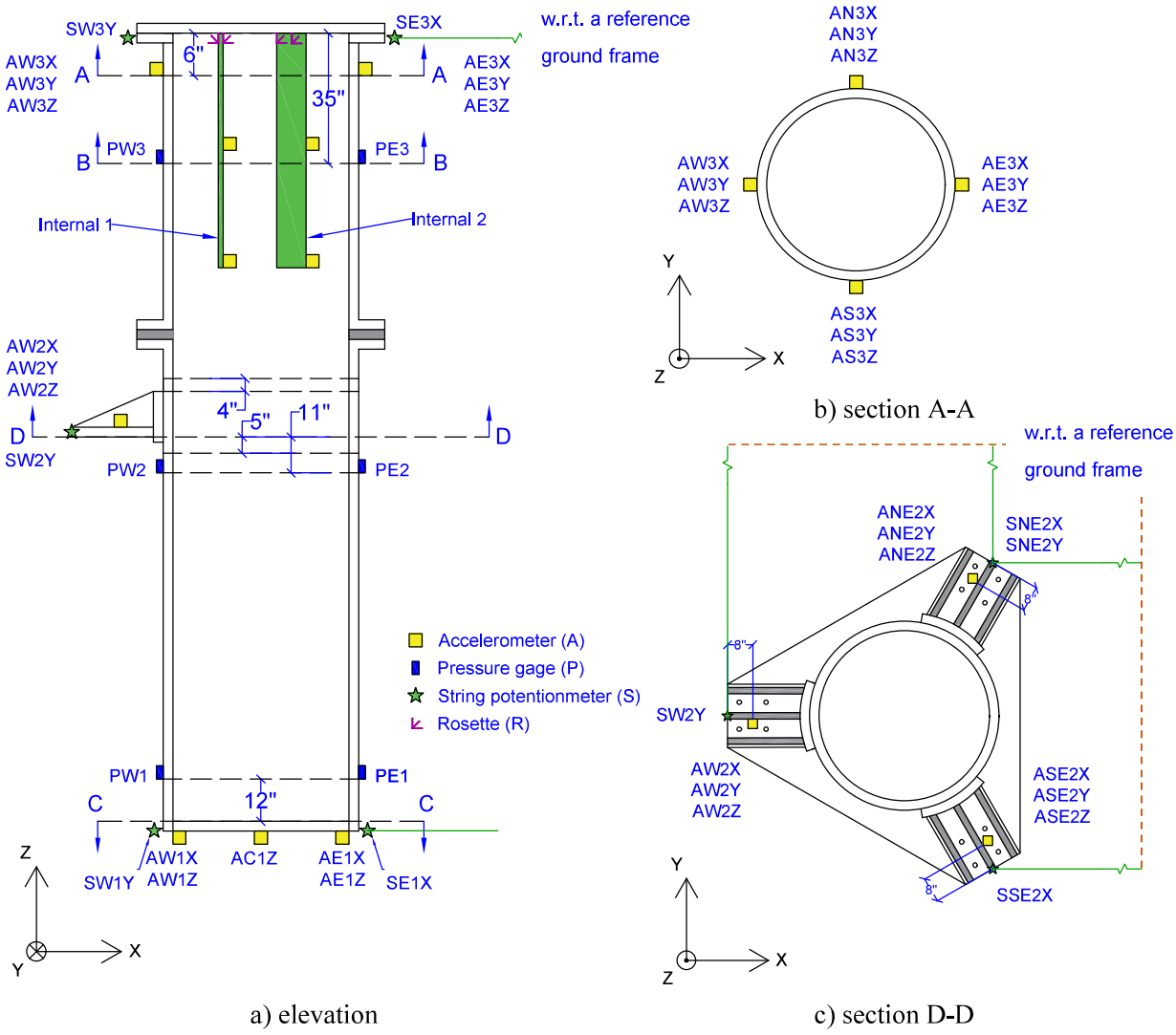

a) elevation

b) section A-A

c) section D-D

Fig. 4 – Instrumentation plan

5. Seismic inputs

Three ground motions from the Pacific Earthquake Engineering Research (PEER) NGA-West 2 ground motion database were used. The motions were selected to have a broad range of frequency content and are listed in Table 2. The time scale of the three components of each ground motion was compressed by a factor of 1.41, consistent with the assumed length-scale factor of 2 for the vessel. Fig.5 presents the 5% damped acceleration response spectra of the time-scaled ground motions. For the testing program, the motions were amplitude scaled to different intensities.

Table 2 – Ground motions for earthquake simulator testing

GM#	Earthquake	RSN#	Peak acceleration		
			Horizontal 1	Horizontal 2	Vertical
1	1987 Edgecumbe	587	0.28	0.24	0.14
2	1987 Superstition Hills	728	0.21	0.23	0.23
3	1898 Loma Prieta	796	0.10	0.20	0.06

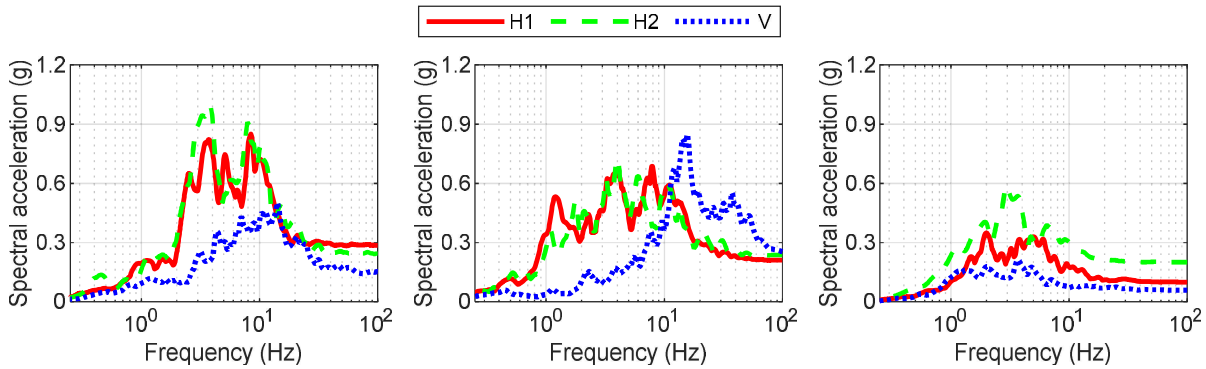

a) GM1 b) GM2 c) GM3

Fig. 5 – Acceleration response spectra of scaled ground motions, 5% damping

6. Test results and discussion

Test results are presented below for two motions: 1) GM1 amplitude scaled to a peak geomean horizontal acceleration of 0.6 g and a peak vertical acceleration of 0.32 g, representing high amplitude shaking, and 2) GM3 amplitude scaled to a peak geomean horizontal acceleration of 0.25 g and a peak vertical acceleration of 0.10 g, representing low-to-moderate amplitude shaking. Table 3 presents the peak geomean horizontal accelerations in the vessel and internals. The amplification of the input motion in the vessel and internals is significant in the non-isolated configuration, with peak geomean horizontal accelerations of more than 2 g at the top and bottom of the vessel, and at the bottom of internals for the high amplitude shaking (i.e., GM1). In the two isolated configurations, the peak geomean horizontal accelerations are substantially reduced with respect to the non-isolated configuration, with reductions by a factor of between 3 and 9 in the vessel and between 2 and 7 in the internals.

Table 3 – Peak geomean horizontal accelerations for vessel and internals

Location	GM1			GM3		
	Non-isolated	SFP-isolated	TFP-isolated	Non-isolated	SFP-isolated	TFP-isolated
Bottom of vessel	2.28	0.33	0.26	0.62	0.18	0.17
Mid-height of vessel	1.11	0.25	0.19	0.51	0.17	0.16
Top of vessel	2.09	0.32	0.26	0.79	0.20	0.18
Bottom of internal 1	3.96	0.82	0.54	1.48	0.67	0.45
Bottom of internal 2	2.04	0.73	0.62	0.87	0.35	0.38

Sample tests results are presented in Fig.6 and Fig.7 for GM1 and GM3, respectively. Results are presented as ratios of spectral response for identical inputs, as a function of frequency, at the bottom, mid-height, and top of the vessel. For frequencies greater than 2 Hz and of interest for the vessel and the internals considered here, the reduction in spectral accelerations afforded by seismic isolation is significant, and by factor of between 2.5 and 7 on average (see black dashed lines in Fig.6 and Fig.7), with greater reductions for higher amplitude shaking (i.e., GM1).

Table 4 presents the peak vertical accelerations in the vessel and the internals for the non-isolated and two isolated configurations. The vertical inputs are not attenuated by the two isolation systems and the peak vertical accelerations in the isolated configurations are similar, as expected, to those from the non-isolated configuration.

Table 4 – Peak vertical accelerations for vessel and internals

Location	GM1			GM3		
	Non-isolated	SFP-isolated	TFP-isolated	Non-isolated	SFP-isolated	TFP-isolated
Bottom of vessel	0.78	0.51	0.51	0.16	0.15	0.16
Mid-height of vessel	0.47	0.34	0.34	0.15	0.14	0.16
Top of vessel	0.77	0.53	0.50	0.16	0.15	0.16
Bottom of internal 1	0.93	0.68	0.60	*	0.18	0.18
Bottom of internal 2	0.80	0.57	0.54	0.18	0.18	0.17

*data not recorded

7. Closing remarks

This paper presents a non-traditional solution for seismic isolation of safety-related equipment inside reactor buildings. A scaled model of a pressure vessel was seismically isolated using Friction Pendulum

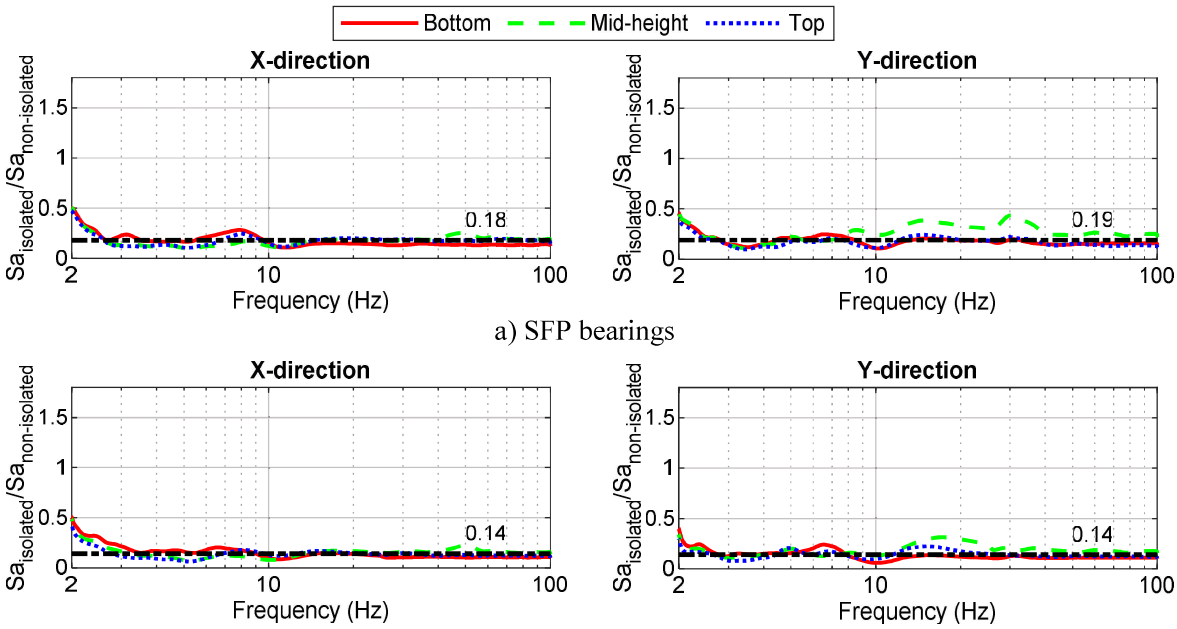

a) SFP bearings

b) TFP bearings

Fig. 6 – Ratio of spectral accelerations in the vessel for GM1

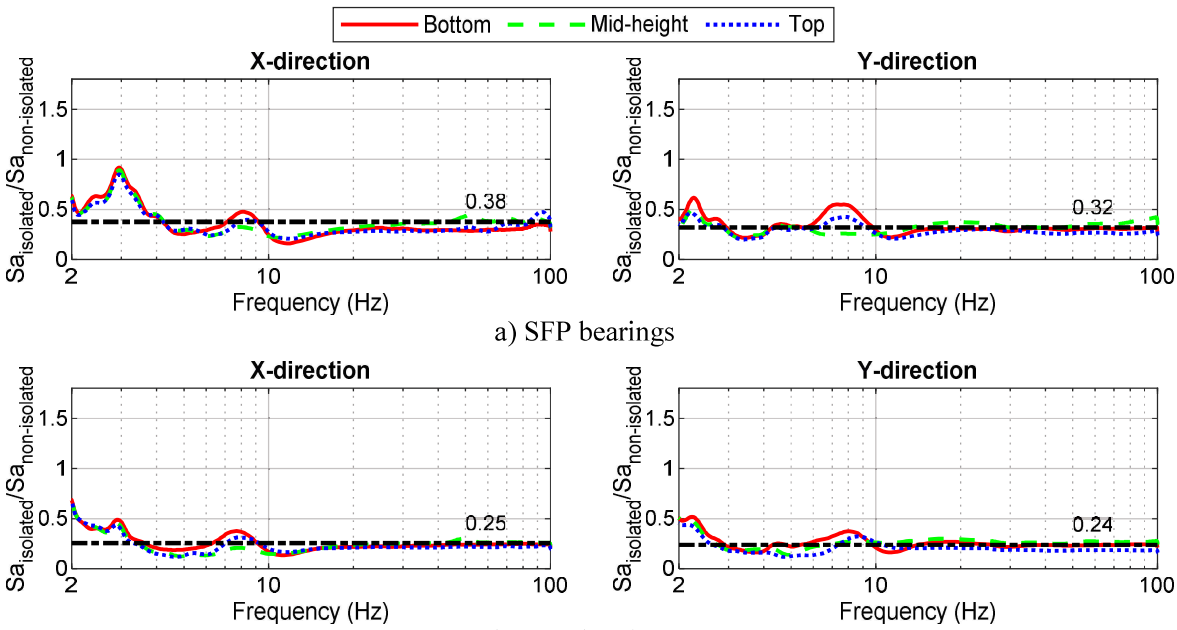

a) SFP bearings

b) TFP bearings

Fig. 7 – Ratio of spectral accelerations in the vessel for GM3

isolators installed at its mid-height and near its center of gravity. Earthquake simulator tests were performed for three configurations: non-isolated, isolated using single concave Friction Pendulum bearings, and isolated using triple Friction Pendulum bearings. The experiment data demonstrated that mid-height isolation is a viable strategy for protecting safety-related equipment with high aspect ratios with reductions in peak horizontal vessel acceleration by a factor of between 4 and 9 for high amplitude shaking (GM1), and 3 and 4 for lower amplitude shaking (GM3). Numerical models, validated using the experiment data, will be used to investigate other non-traditional isolation strategies. The experimental data will be curated and archived at DesignSafe [13].

8. Acknowledgements

The information, data, or work presented herein was funded by the Advanced Research Projects Agency-Energy (ARPA-E), U.S. Department of Energy, under Award Number DE-AR0000978. The views and opinions of the authors expressed herein do not necessarily state or reflect those of the U.S. Government or any agency thereof. The authors thank the technical staff in the Structural Engineering and Earthquake Simulation Laboratory (SEESL) at the University at Buffalo for their assistance in fabricating and instrumenting the test article and executing the earthquake simulator experiments. The authors also thank Earthquake Protection Systems for providing the SFP and TFP bearings at no cost to the project.

9. References

[1] Bolisetti, C., Hoffman, W., Coleman, J. L., Parsi, S. S., Lal, K. M., Whittaker, A. S., Kirchman, P., Bowers, H., and Redd, J. (2020). "Seismic isolation of major advanced reactor systems for economic improvement and safety assurance." INL/EXT-20-59608, Idaho National Laboratory, Idaho Falls, Idaho.

[2] Lal, K. M., Parsi, S. S., and Whittaker, A. S. (2020). "Cost basis for utilizing seismic isolation for nuclear power plant design." Report 03002018345, Electric Power Research Institute, Charlotte, N.C.

[3] Lal, K. M., Parsi, S. S., Charkas, H., Shirvan, K., Cohen, M., Kirchman, P., Kosbab, B., and Whittaker, A. S. (2020). "Reducing the capital cost of nuclear power plants using seismic isolation." *Proceedings: International Congress on Advances in Nuclear Power Plants (ICAPP)*, Abu Dhabi, UAE.

[4] Murota, N., Feng, M. Q., and Liu, G.-Y. (2005). "Experimental and analytical studies of base isolation systems for seismic protection of power transformers." Technical Report MCEER-05-0008, University at Buffalo, State University of New York, Buffalo, NY.

[5] Oikonomou, K., Constantinou, M. C., Reinhorn, A. M., and Yenidogan, C. (2012). "Seismic isolation of electrical equipment - seismic table simulation." *Proceedings: 15th World Conference on Earthquake Engineering (17WCEE)*, Lisbon, Portugal.

[6] Cochran, R. (2015). "Seismic base isolation of a high voltage transformer." *Proceedings: Electrical Transmission and Substation Structures 2015*, Branson, Missouri, 413-425.

[7] Kammerer, A. M., Whittaker, A. S., and Constantinou, M. C. (2019). "Technical considerations for seismic isolation of nuclear facilities." NUREG/CR-7253, United States Nuclear Regulatory Commission, Washington, D.C. (ML19050A422).

[8] American Society of Civil Engineers (ASCE). (2017). "Seismic analysis of safety-related nuclear structures and commentary." *ASCE/SEI 4-16*, Reston VA.

[9] American Society of Civil Engineers (ASCE). (2021). "Seismic design criteria for structures, systems, and components in nuclear facilities." *ASCE/SEI 43-19*, Reston VA.

[10] Mir, F. U. H., Yu, C.-C., and Whittaker, A. S. (2020). "Experiments for validation of FSI models for seismic response of advanced reactor internals." *Proceedings: 17th World Conference on Earthquake Engineering (17WCEE)*, Sendai, Japan.

[11] Fenz, D. M., and Constantinou, M. C. (2008). "Mechanical behavior of multi-spherical sliding bearings." Technical Report MCEER-08-0007, University at Buffalo, State University of New York, Buffalo, NY.

[12] Constantinou, M. C., Whittaker, A. S., Kalpakidis, Y., Fenz, D. M., and Warn, G. P. (2007). "Performance of seismic isolation hardware under service and seismic loading." Technical Report MCEER-07-0012, University at Buffalo, State University of New York, Buffalo, NY.

[13] Rathje, E. M., Dawson, C., Padgett, J. E., Pinelli, J.-P., Stanzione, D., Adair, A., Arduino, P., Brandenberg, S. J., Cockerill, T., and Dey, C. (2017). "DesignSafe: new cyberinfrastructure for natural hazards engineering." *Natural Hazards Review*, 18(3), 06017001.

